THE JOURNAL OF PHYSICAL CHEMISTRY C

Article

pubs.acs.org/JPCC

Indirect-to-Direct Band Gap Crossover in Few-Layer Transition Metal Dichalcogenides: A Theoretical Prediction

Yajing Sun,[†] Dong Wang,*[,†] and Zhigang Shuai*[,†,‡,§]

[†]MOE Key Laboratory of Organic OptoElectronics and Molecular Engineering, Department of Chemistry, Tsinghua University, Beijing 100084, People's Republic of China

[‡]Key Laboratory of Organic Solids, Beijing National Laboratory for Molecular Science (BNLMS), Institute of Chemistry, Chinese Academy of Sciences, Beijing 100190, People's Republic of China

[§]Collaborative Innovation Center of Chemistry for Energy Materials, Xiamen University, Xiamen 351005, People's Republic of China

Supporting Information

ABSTRACT: Layered transition metal dichalcogenides (TMDs) have been found to exhibit the indirect-to-direct band gap transition when exfoliated from bulk to a single monolayer. Through first-principles calculations, we predict that such a transition can happen at bilayer for 2H-WSe_2 and at tetralayer for 2H-WTe_2. We find that the transition can be ascribed to the competition between spin−orbit coupling and interlayer coupling interactions, the former leading to appreciable splittings at the K point and the latter to splittings at the Γ point of the valence band. It is shown that stronger spin−orbit coupling tends to favor transition at a larger number of layers. These results provide insights into the valley degeneracy of the band edges and the valley-dependent optical transitions in few-layer TMDs for quantum control in valley-electronics.

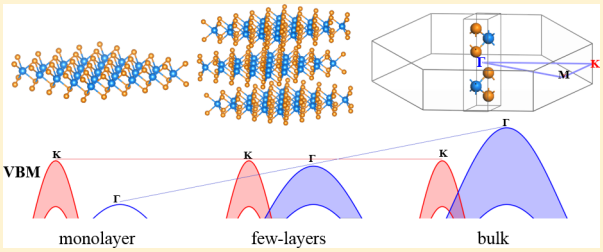

Semiconducting transition metal dichalcogenides (TMDs), MX_2 (M = Mo, W and X = S, Se, Te), have received intense attention for their unique optoelectronic properties, such as the large band gap on−off ratio of FET, the high mobility, and the large exciton binding energy.[1−5] Most interestingly, TMDs share a layered structure, whose optoelectronic properties can be tuned by layer thickness, strain, and alloying.[3,6,7] The atomically thin TMDs can be readily fabricated by either mechanical exfoliation of bulk crystals or chemical vapor deposition (CVD).[6−9] An intriguing finding is the sudden increase of photoluminescence (PL) when these materials are exfoliated to a single monolayer, which has been ascribed to the indirect-to-direct band gap transition, and also confirmed by first-principles calculations.[10−14] For example, bulk MoS_2 has an indirect band gap, while monolayer MoS_2 is a direct band gap semiconductor and recombination of excitons results in strong luminescence.

The indirect-to-direct band gap transition in the monolayer had been believed to be a common property for all of the semiconducting TMDs; until recently, low-temperature measurements of microreflectance (MR) and PL intensity indicate that few-layer $MoTe_2$ behaves differently from other TMDs investigated earlier, such as MoS2 and WS_2.[15] Specifically, their experiment suggests that the indirect-to-direct band gap crossover occurs in the trilayer $MoTe_2$. Because PL is an indirect manifestation of the band structure, here we seek to find from first-principles calculations what makes $MoTe_2$ behave differently and whether such a behavior persists in other TMDs not thoroughly investigated before. In our work, the spin−orbit coupling (SOC) has been included in the self-consistent field calculation, which is found to be essential to understanding PL characteristics of TMDs,[16,17] especially those with heavy elements,[18] but had been overlooked in some earlier investigations.[10,14]

Bulk "2H phase" TMDs (2H-MX_2) are characterized by indirect band gaps between the Γ and Λ points of valence and conduction bands. Here, the letter "H" stands for hexagonal and the digit "2" indicates the number of X−M−X units in the unit cell. When MX_2 is exfoliated to few-layers and the interlayer coupling (ILC) effect is weakened, the Λ energy rises and the Γ energy lowers. If both conduction band minimum (CBM) and valence band maximum (VBM) switch to the K point, the indirect-to-direct band gap transition occurs. We find that such a transition is essentially caused by competition between the SOC and ILC effects. The SOC effect leads to appreciable splittings at the K point of valence band, which are almost independent of the layer thickness. The ILC effect results in energy splittings at the Γ point of valence band as well as at the Λ point of conduction band, while the splittings decrease with the reduction of layer thickness due to the reduced van der Waals interactions. We predict that the indirect-to-direct band gap transition takes place in the bilayer WSe_2 and the tetralayer WTe_2, both of which have heavy elements and strong SOC effect. Our calculations show that bilayer $MoTe_2$ is an indirect band gap semiconductor, but it can

Received: August 30, 2016
Published: September 5, 2016

DOI: 10.1021/acs.jpcc.6b08748
J. Phys. Chem. C 2016, 120, 21866−21870

be turned into a direct one by applying an isotropic tensile strain of 1%. The SOC effect in MoS_2, $MoSe_2$, and WS_2 is not strong enough to compete with the ILC effect, so that the indirect-to-direct band gap transition only occurs when they are exfoliated to a monolayer. The unique valley degeneracy of the band edges and valley-dependent optical selection rules make few-layer TMDs potential materials for valleytronics.

The monolayer X−M−X consists of one hexagonal plane of metal atoms sandwiched between two planes of chalcogens with trigonal plasmatic coordination. We took the lattice parameters of bulk 2H-MX_2 from experiments,[19] and built few-layer MX_2 with at least 20 Å vacuum in the through-plane direction. All of the lattice parameters and atomic positions were optimized by using the PAW method and PBE-D functional with Grimme's dispersion correction as implemented in VASP5.2,[20−22] until the forces were less than 0.005 eV/Å per atom. The plane-wave basis cutoff was 600 eV. The electron density was converged on the *k*-mesh of 8 × 8 × 1, and the band structure along high symmetry directions was calculated. To better illustrate the band structure evolution, absolute energy levels in monolayer and few-layer MX_2 were derived by the vacuum level calibration approach as detailed in our previous work.[23] Among the 2H-MX_2 investigated, WSe_2 exhibits unambiguously the indirect-to-direct band gap crossover in the trilayer. We show in Figure 1 its band structure

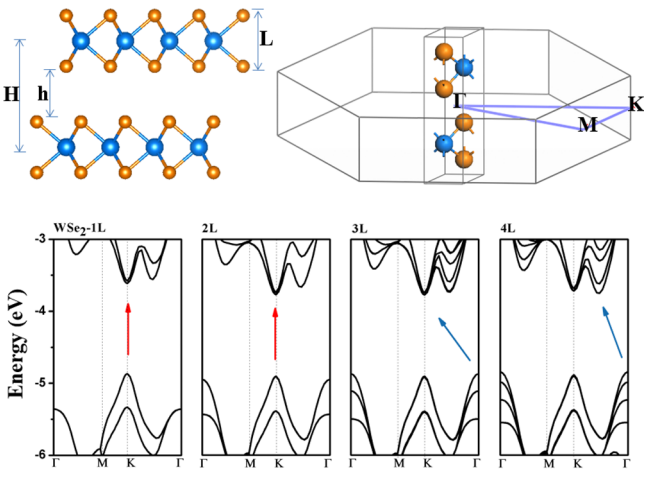

Figure 1. Crystal structure of 2H-TMDs, its first Brillouin zone, and the band structure evolution of WSe_2 as a function of the layer thickness.

evolution as a function of the layer thickness. The typical structural parameters and band gaps of bulk and few-layer WSe_2 have been included in Table 1. There is little change in the W−Se bond length and the Se−W−Se bond angle when it is exfoliated from bulk down to bilayer, but an abrupt increase of the Se−Se distance and the Se−W−Se angle is observed in the monolayer. Bulk WSe_2 is characterized by an indirect band gap from Γ to Λ; see Figure S1. Trilayer WSe_2 is an indirect band gap semiconductor with the K and Λ valley convergence of conduction band (K is 49 meV lower), as well as the K and Γ top convergence of valence band (K is 34 meV lower), resulting in a total of 15 meV difference between the indirect (ΓΛ) and direct (KK) band gap transitions. Both monolayer and bilayer WSe_2 exhibit direct (KK) band gap transitions, but a sharp increase in the band gap is only seen in the monolayer due to the abrupt structural change accompanied by vanishing interlayer interactions.

The competition between K and Γ tops for VBM actually originates from the competition between SOC and ILC effects. By comparing the band structure of monolayer WSe_2 with and without inclusion of the SOC effect (Figure 2), we find that the

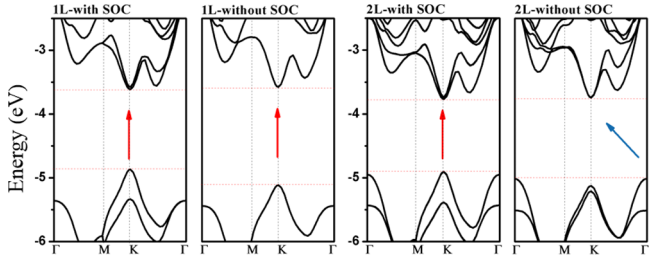

Figure 2. Band structure of monolayer and bilayer WSe_2 with and without the inclusion of SOC.

SOC effect causes an appreciable splitting, 467 meV, at the K point of valence band. This energy splitting is independent of the layer thickness and plays a significant role in the indirect-to-direct band gap crossover in the trilayer WSe_2. In bilayer WSe_2 calculations without inclusion of SOC, the splitting at K is negligible so that VBM remains at Γ; only after the SOC effect is taken into account does it turn into a direct band gap semiconductor (Figure 2). By contrast, the ILC effect causes appreciable splittings at the Γ point of valence band, which are 485, 630, 706, and 875 meV, respectively, in 2L, 3L, 4L, and bulk WSe_2. With the reduction of layer thickness, the splitting decreases gradually, and the Γ top energy lowers by 27 meV when thinned from 4L to 3L, 79 meV from 3L to 2L, and abruptly 410 meV from 2L to 1L due to the electron confinement effect.

By analyzing the projected density of states (PDOS) and charge density distribution at the K and Γ tops of the valence band (Figure 3), we find that these frontier orbitals are mainly constituted by d orbitals of W and p orbitals of Se. The Γ state consists of a d_{z^2} orbital of W and a p_z orbital of Se, so that electrons are delocalized in the out-of-plane direction where interlayer van der Waals interactions exist, whereas the K state

Table 1. Structural Parameters and Band Gaps in Monolayer, Few-Layer, and Bulk WSe_2[a]

WSe_2	*a*/Å	*L*(Se−Se)/Å	*H*(W−W)/Å	*h*(Se−Se)/Å	bond(W−Se)/Å	angle(Se−W−Se)/deg	band gap (K−K, Γ−Λ)/eV
1L	3.319	3.355	N.A.	N.A.	2.546	82.39	1.251, 1.818
2L	3.352	3.331	6.664	3.332	2.554	81.43	1.134, 1.294
3L	3.352	3.330	6.665	3.333	2.554	81.44	1.128, 1.143
4L	3.341	3.337	6.677	3.342	2.535	81.73	1.167, 1.099
bulk	3.352	3.328	6.618	3.290	2.552	81.38	1.123, 0.960

[a] *a* is the lattice constant, *L*(Se−Se) is the height of one layer, and *H*(W−W) and *h*(Se−Se) are the vertical distances of two W and two Se atoms in adjacent layers, respectively.

DOI: 10.1021/acs.jpcc.6b08748
J. Phys. Chem. C 2016, 120, 21866−21870

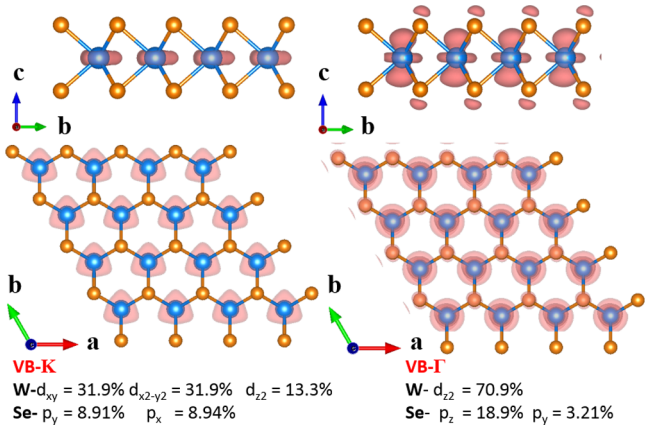

Figure 3. Charge density distribution of monolayer WSe_2 at K and G tops of the valence band for a contour value of 0.10 and 0.03 e/bohr^3, respectively.

is mainly composed of $d_{x^2-y^2}$, d_{xy} orbitals of W and p_x, p_y orbitals of Se, which lack of interlayer couplings. As a result, the Γ energy is sensitive to the ILC effect. With the reduction of layer number, the K energy is only marginally affected while the Γ energy is lowered slowly when exfoliated from bulk to bilayer and significantly from bilayer to monolayer where the interlayer interactions completely disappear. The VBM thus evolves from Γ to K when TMDs are thinned, but at which layer the crossover occurs is determined by the SOC strength, which differs significantly in various TMDs.

The CBM switches from Λ to K in a similar way. The SOC effect leads to trivial splittings at the K valley of the conduction band. Moreover, the K state is composed of W-d_{xy}, $d_{x^2-y^2}$ in-plane atomic orbitals, and its energy remains roughly unchanged when exfoliated from bulk down to bilayer. By contrast, both SOC and ILC effects lead to large splittings at the Λ valley (Figure 2), which is characterized by Se-pz and W-s antibond orbitals. In bulk WSe_2 the CBM is at Λ, but the energy difference between the K and Λ valleys is small, only 31 meV as compared to 132 meV between the K and Γ tops of the valence band. When thinned from tetralayer to monolayer, the Λ energy of the conduction band rises by 201 meV, which is much smaller than the lowering of Γ energy of the valence band (516 meV). The CBM switches from Λ to K in the trilayer WSe_2. The SOC effect in WTe_2 is even larger as manifested by a splitting of 486 meV at the K point of the valence band in the monolayer. The band structure evolution of WTe_2 has been included in Figure S2. It shows that WTe_2 evolves into a direct band gap semiconductor in the tetralayer.

As compared to WSe_2 and WTe_2, MoS_2 and $MoSe_2$ do not have a strong enough SOC effect to compete with the ILC effect. In monolayer MoS_2 and $MoSe_2$, the energy splitting at the K point of valence band is 155 and 188 meV, respectively. These TMDs undergo an indirect-to-direct band gap transition only when exfoliated to a single monolayer where the ILC effect completely vanishes. The band structure evolution of $MoSe_2$ is shown in Figure 4, and that of MoS_2 is supplemented in Figure S3. It has been demonstrated that tensile strains play an important role in tuning the electronic properties of mono- and few-layer MoS_2[24,25] as well as WSe_2.[26] Because the ILC strength can be modulated by inducing the tensile strain in the out-of-plane direction, the indirect-to-direct band gap crossover is expected to be tuned even in few-layer TMDs without heavy elements (tungsten or tellurium), such as MoS_2 and $MoSe_2$. In

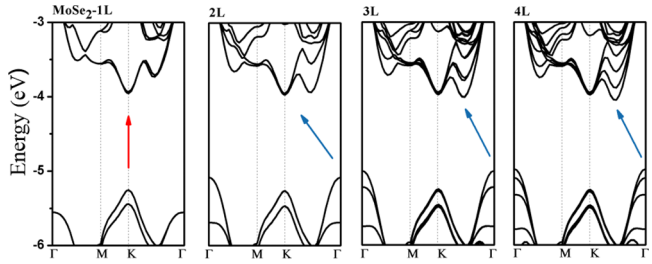

Figure 4. Band structure evolution of $MoSe_2$ as a function of the layer thickness.

the following, we take $MoSe_2$ as an example to illustrate this idea. Bilayer $MoSe_2$ exhibits an indirect band gap transition from Γ to K. The energy difference between the K and Γ tops of the valence band is 182 meV. The tensile strain in the out-of-plane z direction is induced by increasing the distance between the two monolayers, and its magnitude is defined by the ratio of $\Delta H/H_0$, where H represents the Mo−Mo distance in the direction of z. After the tensile strain was applied, the atomic positions other than Mo were fully relaxed. From the band structure evolution of bilayer $MoSe_2$ under the tensile strain (Figure 5), we see that with the strain increasing, the Γ energy

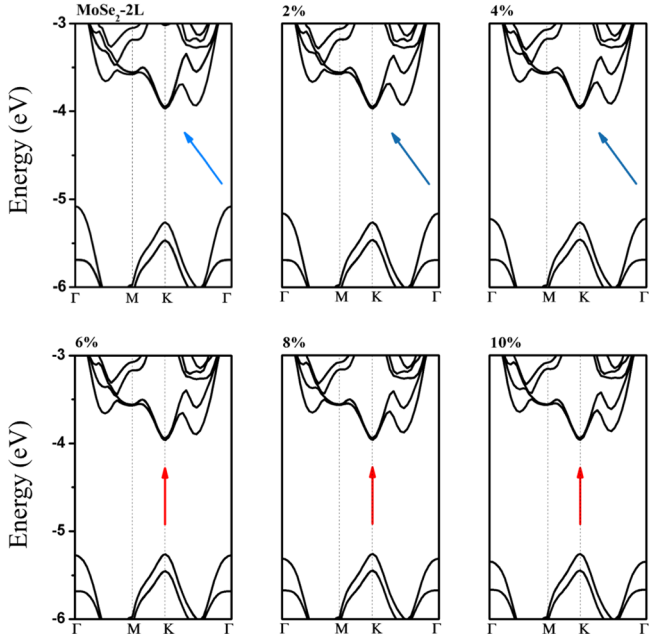

Figure 5. Band structure evolution of bilayer $MoSe_2$ under the tensile strain in the out-of-plane direction.

of the valence band lowers gradually, and the Γ and K energies coincide under the strain of 5%. By applying the tensile strain at above 5%, bilayer $MoSe_2$ is turned into a direct band gap semiconductor, which is desirable for optoelectronic applications.

Although the K splitting of valence band due to the SOC effect is large (430 meV) in monolayer WS_2, it cannot compete with the Γ splitting caused by the ILC effect in few-layer WS_2 (Figure S4). Bilayer WS_2 is an indirect band gap semiconductor with VBM at Γ and CBM at K, and it can be turned into a direct band gap semiconductor by applying above 5% of tensile strain in the out-of-plane direction. Bilayer $MoTe_2$ is also an indirect band gap semiconductor, yet with VBM at K and CBM

DOI: 10.1021/acs.jpcc.6b08748
J. Phys. Chem. C 2016, 120, 21866−21870

at Λ. By applying an isotropic tensile strain of 1% in three dimensions, it can be turned into a direct band gap semiconductor (Figure 6). Our computational result does not

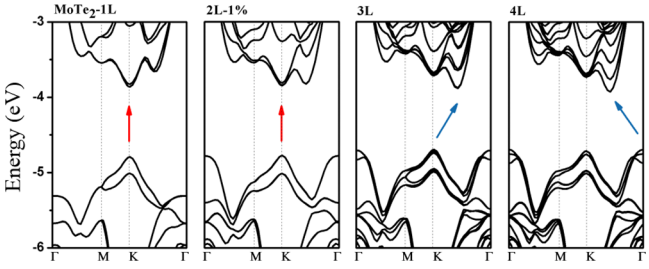

Figure 6. Band structure evolution of $MoTe_2$ as a function of the layer thickness. The isotropic tensile strain of 1% has been applied to bilayer $MoTe_2$.

support the experimental conclusion that bilayer $MoTe_2$ is a direct band gap semiconductor, but we show that the electronic structure of bilayer $MoTe_2$ is susceptible to strain, which could be induced during the exfoliation of bulk $MoTe_2$ and transferring onto the Si substrate. Otherwise, it is possible that the exciton binding energy of K valley is larger than Λ valley so that the direct (KK) band gap transition has strong PL.

In conclusion, we have shown that the indirect-to-direct band gap crossover in few-layer TMDs with heavy elements, such as WSe_2 and WTe_2, takes place even before exfoliation to a single monolayer, which is in contrast to MoS_2 and WS_2 investigated earlier. We demonstrate that the indirect-to-direct band gap transition in these TMDs is essentially a result of competition between the SOC and ILC effects, which respectively lead to appreciable splittings at the K and Γ points of the valence band. We find that the Γ state consists of a d_{z^2} orbital of transition metals and a p_z of chalcogens extending in the out-of-plane direction, so its energy lowers gradually with the reduction of layer thickness. When the SOC effect is strong enough, such as in WSe_2 and WTe_2, the band gap transition takes place at bilayer and tetralayer. We show that by inducing tensile strains in the out-of-plane direction to weaken the ILC effect, the direct band gap transition and enhanced PL quantum yield can be realized in bilayer TMDs without heavy elements, such as $MoSe_2$.

■ ASSOCIATED CONTENT

Supporting Information

The Supporting Information is available free of charge on the ACS Publications website at DOI: 10.1021/acs.jpcc.6b08748.

Band structure evolution of MoS_2, WS_2, and WTe_2; and structural parameters and band gaps of monolayer, few-layer, and bulk MoS_2, $MoSe_2$, $MoTe_2$, WS_2, and WTe_2 (PDF)

■ AUTHOR INFORMATION

Corresponding Authors

*E-mail: dong913@tsinghua.edu.cn.
*E-mail: zgshuai@tsinghua.edu.cn.

Notes

The authors declare no competing financial interest.

■ ACKNOWLEDGMENTS

This work is supported by the National Natural Science Foundation of China (Grant nos. 21273124, 21290190, and 91333202) and the Ministry of Science and Technology of China (Grant nos. 2013CB933503 and 2015CB655002). Computational resources are provided by the Tsinghua Supercomputing Center.

■ REFERENCES

(1) Radisavljevic, B.; Radenovic, A.; Brivio, J.; Giacometti, V.; Kis, A. *Nat. Nanotechnol.* **2011**, *6*, 147−150.
(2) Tan, C.; Zhang, H. *Chem. Soc. Rev.* **2015**, *44*, 2713−2731.
(3) Wang, H.; Yuan, H.; Hong, S. S.; Li, Y.; Cui, Y. *Chem. Soc. Rev.* **2015**, *44*, 2664−2680.
(4) Wang, Q. H.; Kalantar-Zadeh, K.; Kis, A.; Coleman, J. N.; Strano, M. S. *Nat. Nanotechnol.* **2012**, *7*, 699−712.
(5) Chhowalla, M.; Shin, H. S.; Eda, G.; Li, L.-J.; Loh, K. P.; Zhang, H. *Nat. Chem.* **2013**, *5*, 263−275.
(6) Zeng, Z. Y.; Yin, Z. Y.; Huang, X.; Li, H.; He, Q. Y.; Lu, G.; Boey, F.; Zhang, H. *Angew. Chem., Int. Ed.* **2011**, *50*, 11093−11097.
(7) Liu, K. K.; Zhang, W. J.; Lee, Y. H.; Lin, Y. C.; Chang, M. T.; Su, C.; Chang, C. S.; Li, H.; Shi, Y. M.; Zhang, H.; Lai, C. S.; Li, L. J. *Nano Lett.* **2012**, *12*, 1538−1544.
(8) Coleman, J. N.; Lotya, M.; O'Neill, A.; Bergin, S. D.; King, P. J.; Khan, U.; Young, K.; Gaucher, A.; De, S.; Smith, R. J.; Shvets, I. V.; Arora, S. K.; Stanton, G.; Kim, H. Y.; Lee, K.; Kim, G. T.; Duesberg, G. S.; Hallam, T.; Boland, J. J.; Wang, J. J.; Donegan, J. F.; Grunlan, J. C.; Moriarty, G.; Shmeliov, A.; Nicholls, R. J.; Perkins, J. M.; Grieveson, E. M.; Theuwissen, K.; McComb, D. W.; Nellist, P. D.; Nicolosi, V. *Science* **2011**, *331*, 568−571.
(9) Novoselov, K. S.; Jiang, D.; Schedin, F.; Booth, T. J.; Khotkevich, V. V.; Morozov, S. V.; Geim, A. K. *Proc. Natl. Acad. Sci. U. S. A.* **2005**, *102*, 10451−10453.
(10) Splendiani, A.; Sun, L.; Zhang, Y.; Li, T.; Kim, J.; Chim, C.-Y.; Galli, G.; Wang, F. *Nano Lett.* **2010**, *10*, 1271−1275.
(11) Mak, K. F.; Lee, C.; Hone, J.; Shan, J.; Heinz, T. F. *Phys. Rev. Lett.* **2010**, *105*, 136805.
(12) Zhang, Y.; Chang, T.-R.; Zhou, B.; Cui, Y.-T.; Yan, H.; Liu, Z.; Schmitt, F.; Lee, J.; Moore, R.; Chen, Y.; Lin, H.; Jeng, H.-T.; Mo, S.-K.; Hussain, Z.; Bansil, A.; Shen, Z.-X. *Nat. Nanotechnol.* **2013**, *9*, 111−115.
(13) Zhao, W.; Ghorannevis, Z.; Chu, L.; Toh, M.; Kloc, C.; Tan, P.-H.; Eda, G. *ACS Nano* **2013**, *7*, 791−797.
(14) Ellis, J. K.; Lucero, M. J.; Scuseria, G. E. *Appl. Phys. Lett.* **2011**, *99*, 261908.
(15) Lezama, I. G.; Arora, A.; Ubaldini, A.; Barreteau, C.; Giannini, E.; Potemski, M.; Morpurgo, A. F. *Nano Lett.* **2015**, *15*, 2336−2342.
(16) Sun, L.; Yan, J.; Zhan, D.; Liu, L.; Hu, H.; Li, H.; Tay, B. K.; Kuo, J.-L.; Huang, C.-C.; Hewak, D. W.; Lee, P. S.; Shen, Z.-X. *Phys. Rev. Lett.* **2013**, *111*, 126801.
(17) Xiao, D.; Liu, G.-B.; Feng, W.; Xu, X.; Yao, W. *Phys. Rev. Lett.* **2012**, *108*, 196802.
(18) Zhu, Z. Y.; Cheng, Y. C.; Schwingenschlogl, U. *Phys. Rev. B: Condens. Matter Mater. Phys.* **2011**, *84*, 153402.
(19) Al-Hilli, A. A.; Evans, B. L. *J. Cryst. Growth* **1972**, *15*, 93−101.
(20) Perdew, J. P.; Burke, K.; Ernzerhof, M. *Phys. Rev. Lett.* **1996**, *77*, 3865−3868.
(21) Grimme, S. *J. Comput. Chem.* **2006**, *27*, 1787−1799.
(22) Kresse, G.; Hafner, J. *Phys. Rev. B: Condens. Matter Mater. Phys.* **1993**, *47*, 558−561.
(23) Xi, J.; Zhao, T.; Wang, D.; Shuai, Z. *J. Phys. Chem. Lett.* **2014**, *5*, 285−291.
(24) He, K.; Poole, C.; Mak, K. F.; Shan, J. *Nano Lett.* **2013**, *13*, 2931−2936.
(25) Conley, H. J.; Wang, B.; Ziegler, J. I.; Haglund, R. F., Jr; Pantelides, S. T.; Bolotin, K. I. *Nano Lett.* **2013**, *13*, 3626−3630.

DOI: 10.1021/acs.jpcc.6b08748
J. Phys. Chem. C 2016, 120, 21866−21870

(26) Desai, S. B.; Seol, G.; Kang, J. S.; Fang, H.; Battaglia, C.; Kapadia, R.; Ager, J. W.; Guo, J.; Javey, A. *Nano Lett.* **2014**, *14*, 4592−4597.

DOI: 10.1021/acs.jpcc.6b08748
J. Phys. Chem. C 2016, 120, 21866−21870